Geomechanics and Engineering, *Vol. 33, No. 6 (2023) 567-581*
https://doi.org/10.12989/gae.2023.33.6.567

Predicting the rock fragmentation in surface mines using optimized radial basis function and cascaded forward neural network models

Xiaohua Ding[1,2], Moein Bahadori*[3], Mahdi Hasanipanah[4] and Rini Asnida Abdullah[4]

[1]*School of Mines, China University of Mining and Technology, Xuzhou 221116, China*
[2]*State Key Laboratory of Coal Resources and Safe Mining, China University of Mining and Technology, Xuzhou 221116, China*
[3]*Faculty of Engineering, University of Gonabad, Khorasan-e-Razavi, Iran*
[4]*Department of Geotechnics and Transportation, Faculty of Civil Engineering, Universiti Teknologi Malaysia, Skudai 81310, Johor Bahru, Malaysia*

(*Received July 15, 2022, Revised April 28, 2023, Accepted May 2, 2023*)

Abstract. The prediction and achievement of a proper rock fragmentation size is the main challenge of blasting operations in surface mines. This is because an optimum size distribution can optimize the overall mine/plant economics. To this end, this study attempts to develop four improved artificial intelligence models to predict rock fragmentation through cascaded forward neural network (CFNN) and radial basis function neural network (RBFNN) models. In this regards, the CFNN was trained by the Levenberg-Marquardt algorithm (LMA) and Conjugate gradient backpropagation (CGP). Further, the RBFNN was optimized by the Dragonfly Algorithm (DA) and teaching-learning-based optimization (TLBO). For developing the models, the database required was collected from the Midouk copper mine, Iran. After modeling, the statistical functions were computed to check the accuracy of the models, and the root mean square errors (RMSEs) of CFNN-LMA, CFNN-CGP, RBFNN-DA, and RBFNN-TLBO were obtained as 1.0656, 1.9698, 2.2235, and 1.6216, respectively. Accordingly, CFNN-LMA, with the lowest RMSE, was determined as the model with the best prediction results among the four examined in this study.

Keywords: blasting; cascaded forward neural network; fragmentation; prediction models; radial basis function neural network

1. Introduction

Despite the development of mechanical drilling methods in the mining and civil engineering fields, the drilling and blasting method is still widely used as a cost-effective and flexible one (Konya and Walter 1991). According to the literature (Jimeno *et al.* 1992), blasting is a very fast physicochemical operation accompanied by the release of energy in the form of light, shock waves, and gaseous products, with very high temperature and pressure. In each blast operation, only 15 to 30 percent of the energy produced is spent on fragmenting the rock, and the rest of the energy on other phenomena such as ground and air vibration, flyrock, pile movement, and back-break (Hustrulid 1999). After the explosion of the explosive in the blast-holes, the distance between the molecules increases from 10^{-10} meters in the unexploded material to several millimeters in gaseous products in a fraction of a second. This sudden expansion causes a very strong dynamic impact on the rock-wall of the hole (Bhandari 1997). Its pressure is so high that it overwhelms all kinds of rock resistance and causes powdering (Wyllie and Mah 2004). The cylindrical shape around the hole in which the energy of the shock waves is higher than the resistance of the rock mass is called the powdered zone (Dimitraki *et al.* 2019). At the end of the powdered zone, the energy produced by the blast shock waves causes the growth of radial cracks (Hustrulid and Johnson 2008). The length, number, and direction of these cracks depend on the intrinsic properties of the rock mass, stress state, and explosive type (Iverson *et al.* 2010). The range of secondary cylinder with height equal to the height of the hole and the radius equal to the length of the largest crack resulting from the blasting is called radial cracked zone (Johnson 2010). Outside this range, the blast energy is no longer able to fracture the rock mass and only causes elastoplastic deformations and mainly appears in the form of ground vibrations that could expand to several kilometers (Chu *et al.* 2019). In the next step, the gaseous products trapped in the blast-hole leak into the radial cracks and cause them to grow, while simultaneously the compressive shock waves reflected from the free surface are propagated as tensile waves, they form fractures, mostly known as spalling (Hino 1956). The cracks resulting from the spalling phenomenon interfere with the developing cracks by leakage of high-pressure explosive gaseous products, forming a network of fractures (Dare-Bryan *et al.* 2013). When the cracks in this fracture network reach the free surface, along with the gaseous escaping, it causes the fragmented mass to move and collides the moving blocks, and the collision of blocks with the ground surface will cause the final stage of the fragmentation (Shadab Far *et al.* 2019). Then, the pile is located in its final position. In general, the parameters affecting the results of blasting operations are divided into two main categories of

*Corresponding author, Ph.D.
E-mail: moein.bahadori@gmail.com

ISSN: 2005-307X (Print), 2092-6219 (Online)

controllable parameters (the explosive used, burden, distance, sub-drilling, stemming, delay times, direction of blasting, etc.) and uncontrollable ones (rock mass properties, the condition of the discontinuities, groundwater conditions, in situ stresses, the distance of the sensitive structure from the blast site, weather conditions, etc.). In this regard, the designer must design the controllable parameters considering the uncontrollable ones in such a way that an optimal operation result could be achieved (Bahadori *et al.* 2016). Due to the multiplicity of parameters affecting the blasting results and the complexity of their interaction, it will be very difficult to predict the results of the operation (Soltani-Mohammadi *et al.* 2011). Therefore, various researchers have attempted to analyze the relationships between input and output parameters and predict the results of blasting using artificial intelligence methods. Aside from that, the use of artificial intelligence methods has been highlighted in different fields of engineering, which has confirmed the acceptability and reliability of these methods in prediction models (see Asteris *et al.* 2019, 2021a, b, c, d; Apostolopoulou *et al.* 2019; Armaghani *et al.* 2019, 2020a, Cavaleri *et al.* 2019, Chen *et al.* 2019, Li *et al.* 2021, Zhou *et al.* 2021a, b, c, 2022, Bardhan *et al.* 2021, 2022, Le et *al.* 2022, Zeng *et al.* 2021, Huang *et al.* 2022, Skentou *et al.* 2022, Länsivaara *et al.* 2023, Baghbani *et al.* 2023, Kaloop *et al.* 2023). For example, Hasanipanah *et al.* (2016) used two types of artificial neural networks (ANNs) to predict the rock fragmentation in Iranian limestone mines. In another study, by comparing the ANN and multiple regression, Hasanipanah *et al.* (2017) found that ANN can predict particle size distributions with high accuracy. In addition, Esmaeili *et al.* (2015) compared ANFIS and SVM methods and found that ANFIS is more accurate in predicting the size of rocks fragmented by blasting operations. Ebrahimi *et al.* (2016), based on the concept of ANN, used an evolutionary algorithm (the artificial bee colony algorithm) and introduced it as ANN-ABC. They indicated the acceptability of the proposed model in this field. Hasanipanah *et al.* (2018) also employed an intelligent model called PSO-ANFIS and have proven its ability to predict the size distribution of the rock fragments. Gao *et al.* (2018) used Gaussian process regression method in predicting the rock size distribution and compared the results obtained with those of ANFIS, SVM, GPR, and PSO. They found out that GPR method with coefficient of determination (R^2) = 0.948 and mean square error (MSE) = 2.01 achieved higher accuracy. Faraji Asl *et al.* (2018) obtained significant results by combining the firefly algorithm (FFA) with ANN; it recorded an acceptable accuracy (R^2= 0.94 and RMSE = 0.1) in rock fragmentation prediction. Xie *et al.* (2021) combined FFA as an optimizer with different intelligent networks GBM, SVM, GP, and ANN to predict the rock fragmentation. They concluded that the FFA-GBM model provided the highest accuracy in the task defined. An improved boosted generalized additive model (BGAM) model was used by Fang *et al.* (2021) to predict rock fragmentation, and FFA was applied to improving the BGAM performance. In addition, some other models such as SVM and GPR were employed for comparison purposes. According to their results, the BGAM-FFA model predicted the rock fragmentation with the highest accuracy compared to the other models. In the study contacted by Zhou *et al.* (2021b), the genetic algorithm (GA) and FFA were combined with the ANFIS model for the prediction of fragmentation at two quarry mines in Iran. They concluded excellent performance for both GA-ANFIS and FFA-ANFIS models; nevertheless, the former's performance was slightly better than the latter's.

Considering that SAG Mill is used in the Midouk copper mine, Iran, after primary crushing (gyratory crusher) and these mills are basically sensitive to a certain range of particle dimensions (called critical dimensions), predicting the percentage of critical size produced by blasting operation can be effective in reducing the cost of crushing and, consequently, enhancing the profitability degree of the mine.

In this study, to predict the rock fragmentation size in blasting operations, the information of 50 blasting blocks (including uniaxial compressive strength, density, and dynamic stiffness of the rock mass) was recorded, and with the help of several optimized artificial intelligence methods, their effects on the cumulative distribution of particle dimensions (the mean size or d50 and the uniformity index) were evaluated. To do this, the radial basis function neural network (RBFNN) model was optimized with the Dragonfly algorithm (DA) and teaching-learning-based optimization (TLBO). Additionally, the cascaded forward neural network (CFNN) was trained by the Levenberg-Marquardt algorithm (LMA) and Conjugate gradient backpropagation (CGP); then, the obtained models were employed to predict the fragmentation. The main contribution of this study is to develop novel and precise models to predict rock fragmentation, which could also develop the knowledge and insights in this field.

2. Research significance

Blasting is an economical and well-known technique of rock displacement in surface mines to achieve the desired fragmentation. In this regard, an optimum size distribution can directly affect the costs of loading, transportation, and crushing. Therefore, the accurate prediction of fragmentation has critical implications in the entire mining process, for example, the costs of mining and safety issues. Thus, this study attempts to develop new and precise models for the prediction of rock fragmentation.

3. Case study

The Midouk copper mine is located 42 km northeast of Shahrbabak city and 132 km northwest of the Sarcheshmeh mine in Kerman, Iran, with the geographical coordinates of 55° 10' longitude and 30° 25' latitude. The main workshop is at the site of the Midouk mine, which located 7 km northwest of the Midouk village. Fig. 1 shows the geographical location of and the access roads to the mine.

The geological reserve of this deposit is 180 million

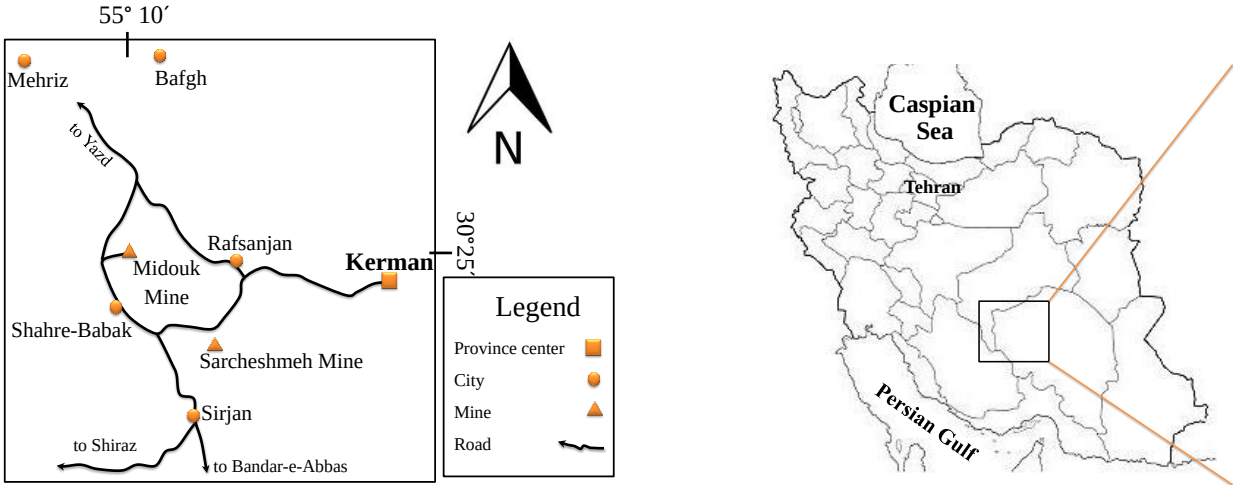

Fig. 1 The geographical location of and access roads to the Midouk copper mine

tons with a grade of 0.83%, from which 144 million tons with a grade of 0.85% can be extracted. Geologically, the mine deposit is in the group of porphyry copper deposits of the monzonite type. The mine cut-off grade is 0.25%, the stripping ratio is 2.4, the overall slope angle of the final pit is 38 degrees, the height of the slopes is 15 m with the width of 9 m, and the slope face angle is 64 degrees. The annual mineral production of mine is planned to be 5 million tons per year, and the mine life is estimated at 29 years based on the extraction plans (Bahadori *et al*. 2016).

As the width and height of the operational benches in the mine are 20 m and 15 m, respectively, the blast holes are drilled by 12 drilling machines TREX, Ingersoll Rand, and T4 with diameters of 150 mm to 200 mm with a depth of 17 m (including 2 m sub-drilling) in a zig-zag form with the 5×6.5 m, 5.5×7 m, and 6.5×8 m patterns. Depending on the water conditions of the blast holes, ANFO or Emolan charges are selected as the main charge, and the NONEL (Non-Electric initiating system) or Cordtex systems with a delay times of 25 ms, 42 ms, 50 ms, and 65 ms are used. It is worth noting that for blasting blocks that use the Emolan (which is a stronger charge in comparison with ANFO), the dimensions of the larger geometry of blasting pattern are selected (Bahadori *et al.* 2016).

The production process of the Midouk plant includes crushing, material transfer units, flotation material classification, and dewatering, which leads to the extraction of concentrate as a final product. The extracted sulfide ores are crushed to a size of less than 20 cm in a gyrator crusher and then entered into the SAG mill and two ball mills with nominal capacity of 806 and 781.5 ton per hour, respectively. Rocks with dimensions less than 1000 microns that come out of the SAG mill are introduced into the primary cyclone by cyclone pump, while the coarse rocks enter the ball mills (which are in the closed-circuit). The product of the ball mills also enters the cyclone pump tank and is pumped back to the primary separator hydro cyclone. The diameters of these balls equal 30, 50, 60, 80, 100, and 125 mm (Rahimi and Abdollahzade 2020).

To divide the rock masses in the Midouk copper mine into special zones, a set of field surveys, laboratory tests, and changes of the trends in the different units of mine and processing plant were evaluated and recorded. For this work, four main categorized studies were conducted for 50 blasting blocks containing geo-structural surveys (including joint conditions), rock mechanics experiments (density, uniaxial compressive strength, and dynamic stiffness), analysis of size distribution of rock fragments, and tracking the changes in the consumption power of the processing unit considering blending quality for the input feed. Table 1 summarizes the recorded values from the field measurements and laboratory experiments. Note that the database includes 50 datasets; and the train and test data were randomly selected with a ratio of 80% and 20%, respectively, of the entire data.

Table 1 Summary of measured values from the field surveys and laboratory tests of the site

Parameter	Symbol	Unit	Min	Max
Hole diameter	ϕ	mm	152	203
Hole depth	h_d	m	16.83	18.33
Specific charge	SC	kg/m^3	0.27	0.81
Burden	B	m	3.4	6.8
Spacing	S	m	5.87	8.2
Stemming	St	m	4.5	9.0
Sub-drilling	Su	m	1.83	3.33
Density	ρ_r	kg/m^3	2235	2575
UCS	σ_c	MPa	10	90.8
Dynamic hardness	-	-	20	112
Mean size of rock fragments	d_{50}	cm	2.21	18.72
Uniformity coefficient	n	-	3.2	16.45

To recognize the main joints in the mine region, the scan line technique was used and for any blasting block two stations of measurement is conducted. The servocontrol unit of the UCS (Unconfined Compressive Strength) test and SMC test unit in the Midouk copper mine are used to measure the strength parameter of the rock specimens.

According to field measurements, the main joints in the

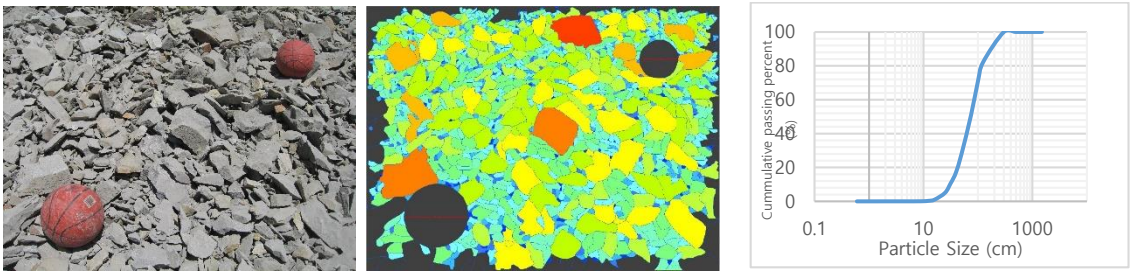

Fig. 2 Analysis of the size distribution of rock fragments using WIp-frag Software

mine area are vertical joints with north-south and east-west directions, which intersect with the category of oblique and horizontal joints. The spacing of the joints is very close (in some cases less than 2 cm), and their density and frequency are very high in some areas.

As shown in Fig. 2, this analysis was conducted using the Wip-frag software with the help of two scales to remove the depth and the tilting effects. To avoid missing data, images were taken perpendicular to the pile of rock fragments and each pile was divided into three parts along with the loading and hauling process. For any part, at least five images were analyzed, and the average of all results was considered as the size distribution of rock fragmentation by blasting.

To determine the dynamic hardness of rock material in the area of the Midouk copper mine, the SAG Mill Comminution (SMC) test method was used. This test is a short method of drop weight test, which was pioneered by Morrell (2004). The only difference between the two methods is in the tested samples. In this study, due to the limitations of devices available in the laboratory of the Midouk copper mine processing unit, the SMC test was used. The t10 index determination experiment, known as the drop weight method, is a practical method for determining the strength of different materials for the given range of dimensions, and the results are used in numerical and mathematical modeling of SAG mills and AG mills. In this method, the size distribution of fragments for a specific sample is determined after the impact of a heavy object.

The drop weight test is a suitable method for determining the properties of ores crushed in SAG mills and AG as well as their resistance to impact. The purpose of this experiment is to determine the rock material fracture characteristics for different levels of impact energy (Napier-Munn *et al.* 1996). Table 2 presents the mean size (d_{50}) and the uniformity coefficient of the size distribution (n) for fragmented rocks, charge type, specific charge, and the dynamic hardness of rock material for the selected blasting patterns in the Midouk copper mine. It is worth noting that the d_{50} and n are obtained from the best adaptation of the experimental KCO (Kuznetsov-Cunningham-Ouchterlony) function to the data obtained from image processing.

To determine the share of critical sizes produced in rock blasting, the d_{50}, the n parameters, and the size distribution curves for the rock fragments at the selected stations were evaluated. Among the existing experimental fragmentation relationships (including Rossin-Ramler, SveDeFo, TCM, CZM, KCO, and Tanh relationships) using the Solver plug-in in Microsoft-Excel software, the d_{50} and the n parameters were determined, provided that the regression value between the obtained experimental relationship and the field data maximizes (Kanchibotla *et al.* 1999, Djordjevic 1999, Ouchterlony 2005, Bahadori and Bakhshandeh Amnieh 2018). This operation was repeated for the case where the aim is minimizing mean square error, although no change in results was observed. Based on the obtained values, the KCO function in most cases (33 out of 50 cases) delivers the best adaptation to the image analysis of the rock fragmentation by blasting in the Midouk copper mine.

4. Methods

4.1 Radial basis function neural network

The Radial basis function neural network (RBFNN) is one of ANNs successfully applied to distinct modeling cases. The RBFNN is characterized by its sole hidden layer, which is located between the input and output layers (Elsharkawy 1998). The hidden layer has a substantial contribution in the accuracy of the RBFNN model as the data is transformed and processed at its nodes by applying nonlinear transformation functions, namely radial basis function types such as the Gaussian function. This sort of functions involves two main control parameters: the spread coefficient (σ^2) and the center (c_i). These two parameters are vital in the calculations carried out. In this context, the Euclidian norm is considered for assessing the positions of the input vectors with respect to the center of this function, as follows (Haykin 1999)

$$\vec{a}_c = 2v \times \vec{\omega} \tag{1}$$

where the dimension of the system and the centers are denoted by D and c_{ij}, respectively. Then, the output of the above-formula is applied to the Gaussian function, as shown below (Nait Amar *et al.* 2021a)

$$\Phi(e) = exp\left[\frac{e^2}{2\sigma^2}\right] \tag{2}$$

where Φ denotes the Gaussian function, and σ^2 and e represent the spread coefficient and the Euclidian distance, respectively.

Finally, the outputs of the paradigms are obtained by applying the following formula

$$o_j = \sum_{i=1}^{m} w_{ij}\, \Phi_i(e) + b_i \text{ , } i = 1, \ldots, m \text{ and } j = 1, \ldots, N \quad (3)$$

where m and N signify the number of neurons in the hidden layer and the data size, respectively, o_j is the output with the index j, w_{ij} is the weight linking the hidden neuron i to the output layer, and b_i is the bias term.

To ensure a robustness in the results generated by the RBFNN model, its main control parameters, namely the number of nodes in the hidden layers as well as the spread coefficient of the Gaussian function, should be chosen properly. To this end, we proposed to evolve two rigorous metaheuristic algorithms to optimize the aforementioned control parameters of RBFNN in this study. These two algorithms are dragonfly (DA) and teaching learning-based optimization (TLBO).

4.2 Cascaded forward neural network

Cascaded forward neural network **(**CFNN) is another type of ANN, which is known by the accuracy of its results despite the high degree of complexity of some of the systems to which this technique is applied (Nait Amar *et al.* 2020, 2021b). This advantage is generated by the CFNN structure that has the peculiarity in the connections between the layers. In this context, the cascade form is used to connect between the neurons of the different layers (Nait Amar *et al.* 2021c). This form allows to connect the neurons of a given layer to the neurons of the previous ones. In terms of design, CFNN includes an input layer, one or more hidden layers, and an output layer (Abujazar *et al.* 2018, Zimmermann and Mattedi 2020). Generally, the trial and error method is the technique applied to find the appropriate number of hidden layers, their neuron numbers, and their activation functions.

CFNN goes through a vital step to complete the best predictions. This step is the learning phase that aims to get the best connections (weight values) that result in minimizing the square error between the observations and the results of the paradigm (Abujazar *et al.* 2018, Zimmermann and Mattedi 2020). In this study, the Levenberg-Marquardt (LM) and conjugate gradient backpropagation with Polak-Ribiére (CGP) algorithms, which are of the backpropagation type, were applied to the learning phase of the CFNN model.

4.3 Optimization techniques

4.3.1 Levenberg-Marquardt algorithm

Levenberg-Marquardt algorithm (LMA) is one of the well-known approaches to non-linear least square based tasks (Benamara *et al*. 2020). LMA has gained importance in the training phase of many feedforward neural networks (FFNNs) such as multilayer perceptron (MLP) and CFNN thanks to its acceptable performance and low-cost calculability efforts (Simon 2009, Nait Amar and Zeraibi 2019). The main calculation steps in this algorithm have several points in common with those of the Newton's method. Nevertheless, some differences can be distinguished, including the introduction of a regularization parameter to improve the quality of the calculations and the expression applied to the Hessian matrix estimation, which is given as follows (Simon 2009)

$$H = J^T J \quad (4)$$

where J stands for the Jacobian matrix and T signifies the matrix transposition operator.

During the calculation steps performed in LMA, the step of approximating the Hessian matrix is followed by the substitution of the latter in the main formula of Newton's method. This can be illustrated by Eq. (5): (Simon 2009)

$$\mathrm{w_{k+1}} = \mathrm{w_k} - (\mathrm{H} - \lambda \mathrm{I})^{-1} \times \mathrm{J^T e} \quad (5)$$

where *e* stands for the error vector, λ is the regularization parameter, and *k* and *w* denote the iteration and weights, respectively.

4.3.2 Conjugate gradient backpropagation with Polak–Ribiére

Conjugate gradient backpropagation with Polak–Ribiére (CGP) is another robust approach to optimizing the weight and bias values of FFNN types. This algorithm involves the calculation of the derivatives of the considered fitness function with respect to the weight and bias terms (Gupta *et al.* 2011). The update of these terms is done using the following formula (Sui Kim *et al.* 2020)

$$x_{k+1} = x_k + c_k \times P_k \quad (6)$$

where k and x denote the iteration and variables (weights, bias), respectively, c_k is a parameter selected to decrease the gradient, and P_k represents the search direction which is initially equal to $-g_0$ where g is the gradient, while for the other iterations, it is assessed using the following formula (Gupta *et al*. 2011)

$$P_k = -g_k + P_{k-1} \times z \quad (7)$$

where g is the gradient, and z is obtained using the expression below (Gupta *et al*. 2011)

$$z = \frac{(g_k - g_{k-1})' \times g_k}{ns} \quad (8)$$

where ns represents the norm square of the gradient at $(k-1)$.

4.3.3 Dragonfly algorithm

The Dragonfly algorithm (DA) is a swarm-inspired optimization algorithm, which was introduced by Mirjalili (2016). DA was inspired by dragonflies' behavior and their hunting process (Moayedi *et al*. 2021). DA proceeds to the optimization process by implementing five steps that mimic the hunting mechanism of dragonflies in nature. These steps and their corresponding mathematical formulas are stated below (Mirjalili 2016)

- Separation: $\mathrm{S_k} = -\sum_{\mathrm{k=0}}^{\mathrm{N}} \mathrm{X} - \mathrm{X_k}$
- Alignment: $\mathrm{A_k} = -\frac{\sum_{\mathrm{k=0}}^{\mathrm{N}} \mathrm{V_k}}{\mathrm{N}}$
- Cohesion: $\mathrm{C_k} = -\frac{\sum_{\mathrm{k=0}}^{\mathrm{N}} \mathrm{X_k}}{\mathrm{N}} - \mathrm{X}$
- Attracting to prey: $\mathrm{F_k} = \mathrm{X^+} - \mathrm{X}$
- Distraction from the enemy: $\mathrm{E_k} = \mathrm{X^-} - \mathrm{X}$

where N is the size of the population, X and V stand for the position and the velocity of the dragonfly, respectively,

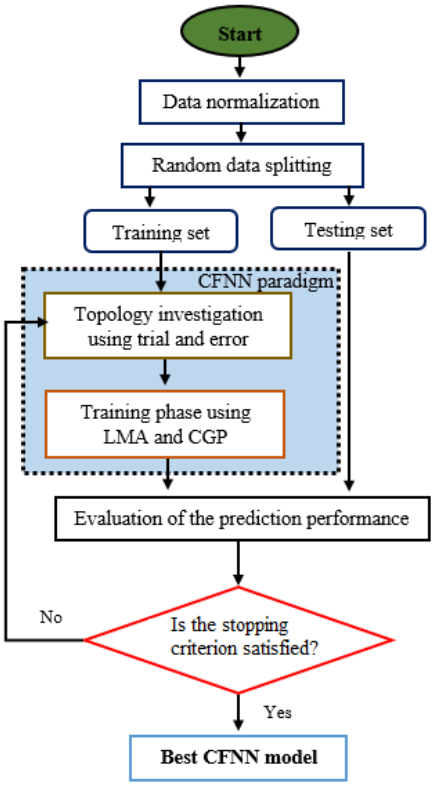

Fig. 3 The proposed workflow for implementing the CFNN schemes

while X^- and X^+ represent the positions of the enemy and food source, respectively.

The exploitation of the above-stated equations allows DA to update the positions using the following equation (Mirjalili 2016)

$$X_{i+1} = X_i + \Delta X_{i+1} \tag{9}$$

where ΔX_{i+1} is calculated as follows (Mirjalili 2016)

$$\Delta X_{i+1} = (sS_k + aA_k + cC_k + fF_k + eE_k) + w\Delta X_i \tag{10}$$

with

$$e = 0.1 - i \times \left(\frac{0.1}{\frac{t}{2}}\right) \tag{11}$$

$$w = 0.9 - i \times \left(\frac{0.9 - 0.4}{t}\right) \tag{12}$$

where i and t are the iteration and the total number of iterations, respectively, a, c, and s are random values in the interval [0 − 2e], and f signifies a random value from [0 − 2] (Mirjalili *et al.* 2020).

4.3.4 Teaching-Learning-Based Optimization

The Teaching-Learning-Based Optimization (TLBO) algorithm is among the population-based algorithms, which has gained great consideration due to its efficiency in resolving many kinds of optimization problems. TLBO was proposed by Rao *et al.* (2011) for emulating the standard school learning procedure involving two stages: the teacher and the learner stages. The first stage comprises improving the learning ability of the class. This phase is carried out by designating the smartest student in the class as the teacher, while the other students attempt to develop their capabilities with respect to the difference between the teacher and the mean of the group. Mathematically, this step is described as shown below (Rao *et al.* 2011, Cheng and Prayogo 2017)

$$X_{i\,new} = X_{i\,old} + r \times \left(X_t - T_f \times \bar{X}\right) \tag{13}$$

where X_t and $\bar{X}$ denote the position of the teacher and the mean value of the class, respectively, r is a random value within the interval [0, 1], and T_f represents the teaching factor.

Then, during the second stage of TLBO, i.e., the learner stage, each student attempts to enhance their skills by interacting with another student randomly chosen from among the class. If this chosen student is smarter than the student in question, the latter will change his position towards this chosen student. Otherwise, the position will not be updated. The mathematical application of this phase is given below (Rao *et al.* 2011, Cheng and Prayogo 2017)

$$X_{i\,new} = \begin{cases} X_{i\,old} + r \times \left(X_i - X_j\right) \; if \; f(X_i) < f(X_j) \\ X_{i\,old} + r \times \left(X_j - X_i\right) \; if \; f(X_j) < f(X_i) \end{cases} \tag{14}$$

where is a random value within the interval [0, 1]. The new positions are kept if they result in better function values.

5. Implementation procedure

Figs. 3 and 4 depict the workflows considered for implementing the proposed machine learning-based models

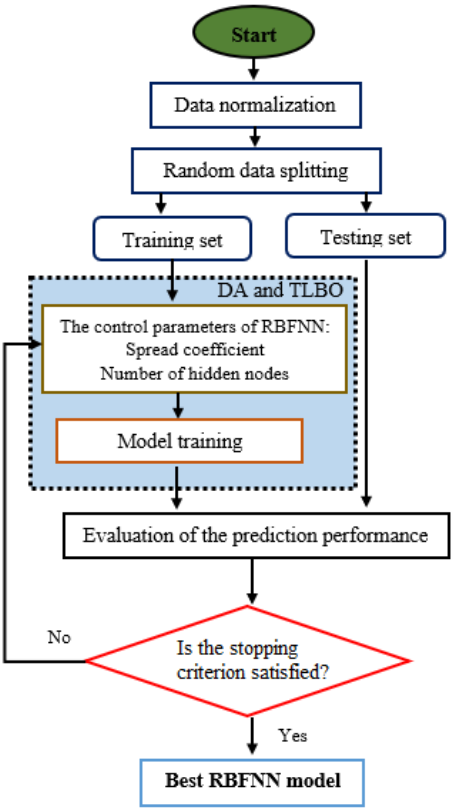

Fig. 4 The proposed workflow for implementing RBFNN schemes

for predicting d_{50}. As stated earlier, these models are CFNN-LMA, CFNN-CGP, RBFNN-DA, and RBFNN-TLBO. As stated in the workflows of Figs. 3 and 4, the data collected from the published literature was normalized. The following formula was used to normalize the amassed database

$$X_N = \frac{2(X_i - X_{min})}{(X_{max} - X_{min})} - 1 \quad (15)$$

where X and X_N stand for the variable and its normalization, respectively, while X_{max} and X_{min} denote the maximum and minimum values of the variable, respectively.

Before proceeding to the training phase, the normalized database was divided randomly into two data sets, namely the training set (80% of the gathered points) employed during the development of the paradigms, and the testing set (20% of the gathered points) applied to validating the established ML-based paradigms. As mentioned in the previous section, the main control parameters of CFNN and RBFNN should be investigated adequately in order to obtain desirable predictions. For the case of CFNN, the trial and error technique was used to inspect the proper topology of the model. This step was followed by the optimization of the weight and bias values of the CFNN schemes using LMA and CGP algorithms. For the RBFNN model, DA and TLBO algorithms were implemented for examining the adequate number of hidden nodes and the spread coefficient values. During the optimization of the RBFNN control parameters using these two algorithms, the population size was set to 50 and the total number of iterations to 100.

6. Results and discussion

The following statistical functions are applied to assessing the prediction performance of the aforementioned models (Armaghani *et al.* 2020a, b, Bai *et al.* 2021, Liu *et al.* 2021)

1. Average Absolute Relative Deviation (AARD).

$$AARD\% = \frac{1}{N}\sum_{i=1}^{N}\left|\frac{d50_{i_{obs}} - d50_{i_{pred}}}{d50_{i_{obs}}}\right| \times 100 \quad (16)$$

2. Coefficient of Determination (R^2).

$$R^2 = 1 - \frac{\sum_{i=1}^{N}\left(d50_{i_{obs}} - d50_{i_{pred}}\right)^2}{\sum_{i=1}^{N}\left(d50_{i_{pred}} - \overline{d50}\right)^2} \quad (17)$$

3. Root Mean Square Error (RMSE).

$$\mathrm{RMSE} = \sqrt{\frac{1}{N}\sum_{i=1}^{N}\left(d50_{i_{obs}} - d50_{i_{pred}}\right)^2} \quad (18)$$

where the subscripts obs and pred signify the observed and predicted values of d_{50}, respectively, $\overline{d50}$ represents the average value of d_{50}, and N is the number of points.

In addition to the statistical assessment, graphical techniques such as Taylor's (2001) diagram, cross plot, and error distribution diagrams were drawn for the visual evaluation of the prediction performance of the newly proposed paradigms.

The main control parameters of the newly suggested CFNN- and RBFNN-based paradigms are stated in Tables 2 and 3, respectively.

Table 2 The main control parameters of the CFNN models

Factor	CFNN-LMA	CFNN-CGP
Number of hidden layers	3	3
Number of neurons in the hidden layers	11-10-9	11-11-9
Activation functions in the hidden layers	Tansig	Tansig

Table 3 The main control parameters of the RBFNN models

Factor	RBFNN-DA	RBFNN-TLBO
Number of hidden nodes	15	14
Spread coefficient values	1.4780	1.4267

Fig. 5 shows the cross plots exhibiting the predictions of the proposed ML-based models versus the observed values of d_{50}. This kind of graphical analysis allows the examination of the prediction performance by comparing the nature of models' estimation around the unit-slope line which is the reference of the best paradigm that can exist.

These plots indicate that the d_{50} values generated by the proposed ANN schemes are acceptable enough as the latter fall on a unit-slope straight line.

To confirm this claim, the error between the observed and estimated values of d_{50} versus the observed d_{50} values is depicted in Fig. 6 for the RBFNN-DA, RBFNN-TLBO, CFNN-LMA, and CFNN-CGP models. The errors shown in these distributions correspond to the difference between the observed and predicted values of d_{50}. As can be seen, the errors associated with the models' predictions lie in somewhat small range, while a great part of the points is located around the zero-error line. The error distribution diagrams shown in Fig. 6 prove that the predictions of the implemented ML-based paradigms are in satisfactory agreement with the real values of d_{50}.

Table 4 shows the statistical criteria, namely AARD, R^2, and RMSE for all groups of data, i.e., training, test, and all data. In addition, Fig. 7 displays the values of measured and predicted values obtained from the predictive models for all data used in the modeling. Also, Fig. 8 displays the Taylor diagram that joins together various statistical functions according to Table 4, and although the satisfactory values of the reported statistical functions of the implemented models was obtained, it can be deduced that CFNN schemes outperform the RBFNN schemes. This conclusion can be drawn from the Taylor diagram illustrated in Fig. 8 where it can be seen that CFNN-LMA and CFNN-CGP exhibit better performance as these paradigms are located in the nearest position around the arc showing the real observation values of d_{50}. Furthermore, and by taking a deeper analysis on the reported results in Table 4, and Figs. 7 and 8, it can be said that CFNN-LMA model is the best paradigm for predicting the d_{50} values with an overall R^2 value of 0.9514.

Fig. 9 illustrates the cumulative frequency of absolute errors noticed in the predictions of the newly implemented CFNN-LMA model. As can be observed, our best paradigm, namely CFNN-LMA can estimate the d_{50} value of more than 90% of the data with an error value of 2 and more than 75% of the data with an error value of 1. This figure

Table 4 Statistical evaluation of the implemented CFNN and RBFNN schemes

Model	Sorting of data	AARD (%)	R^2	RMSE
CFNN-LMA	Training data	12.8802	0.9518	1.1666
	Test data	16.8035	0.9496	1.0656
	All data	13.6648	0.9514	1.1471
CFNN-CGP	Training data	10.4873	0.9577	1.0029
	Test data	25.7872	0.9355	1.9698
	All data	13.5473	0.9431	1.2573
RBFNN-DA	Training data	13.6789	0.8645	1.2260
	Test data	40.1037	0.7982	2.2235
	All data	18.9639	0.8411	1.4803
RBFNN-TLBO	Training data	12.2915	0.9177	1.0959
	Test data	13.9882	0.7127	1.6216
	All data	12.6308	0.8922	1.2194

confirms again the reliability of CFNN-LMA in estimating d_{50}.

Lastly, the relevancy factor (r) was calculated in order to assess the impact degree of the different variables on the values of d_{50}. This factor can be determined using the following equation (Chen *et al.* 2014)

$$r(I_j, O) = \frac{\sum_{i=1}^{N}(I_{j,i}-\bar{I_j})(O_i-\bar{O})}{\sqrt{\sum_{i=1}^{N}(I_{j,i}-\bar{I_j})^2 \sum_{i=1}^{N}(O_i-\bar{O})^2}} \quad (19)$$

where the variable index and data index are represented by j and i, respectively, I and $\bar{I}$ denote the variable and its average value, respectively, and O and $\bar{O}$ represent the predicted value of the output and its average, respectively.

Fig. 10 displays the relative effect of the input parameters on the values of d_{50}. As can be seen, UCS, point load, hardness value, and density are the factors of highest impact on the d50 values, while the other parameters come after with impacts lower than 10%.

7. Conclusions

A crucial subject after each blasting operation is the quality of the fragmentation. An optimum fragmentation can optimize the overall mine/plant economics. Therefore, the prediction and evaluation of fragmentation with a high degree of accuracy is a task of high necessity. With the aim of the prediction of fragmentation, four advanced artificial intelligence models, i.e., CFNN-LMA, CFNN-CGP, RBFNN-DA, and RBFNN-TLBO, were proposed in this study. The performance of these models were then evaluated through three statistical functions: AARD, R^2, and RMSE. Some conclusions were drawn as follow: (1) Comparison results demonstrated that the CFNN-LMA model outperformed the other three models in terms of predicting the rock fragmentation. The amount of R^2 obtained from the CFNN-LMA, CFNN-CGP, RBFNN-DA, and RBFNN-TLBO models were 0.9496, 0.9355, 0.7892, and 0.7127, respectively, which indicates the better performance of CFNN-LMA

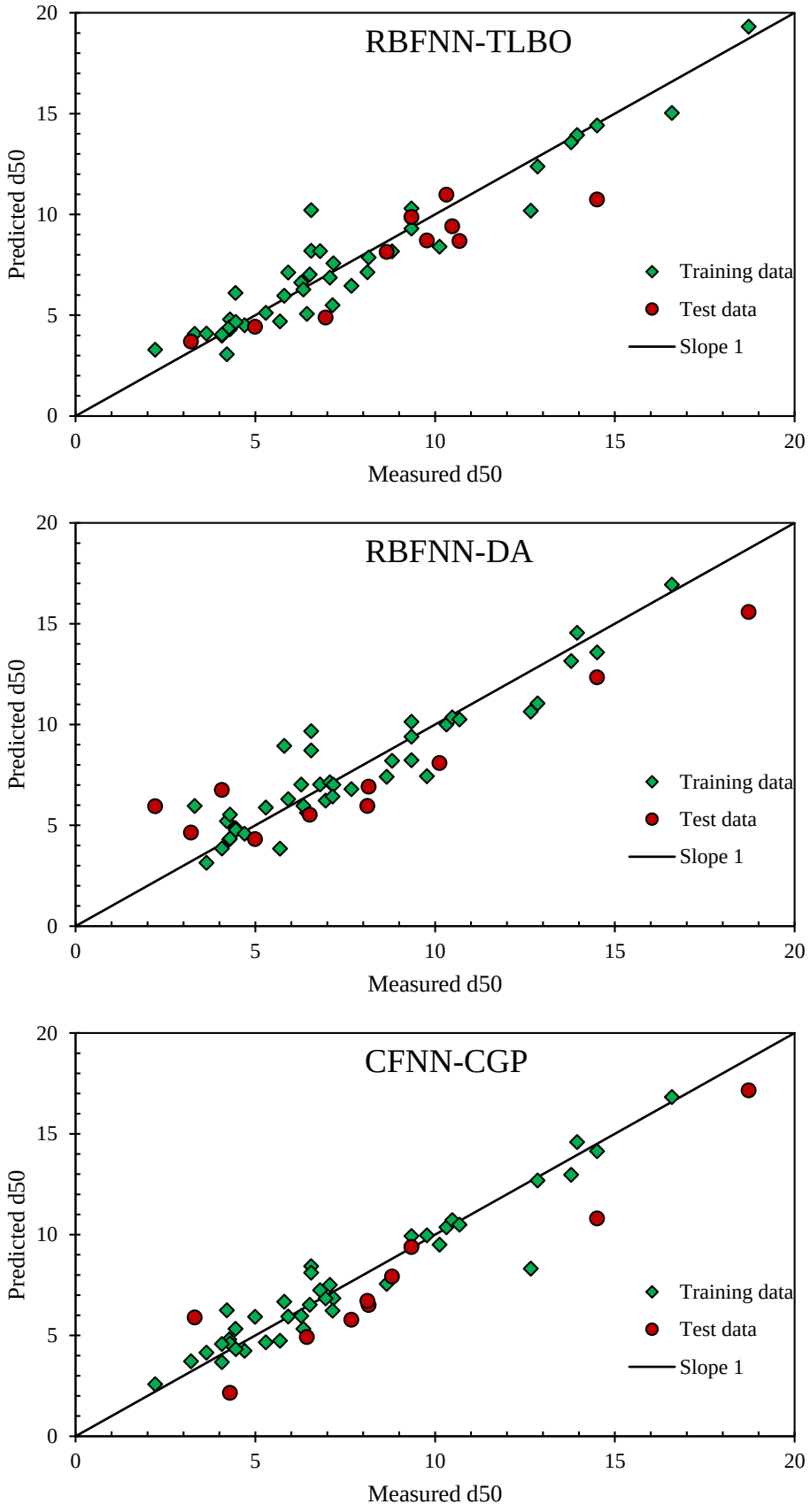

Fig. 5 Cross plots of the implemented CFNN and RBFNN schemes

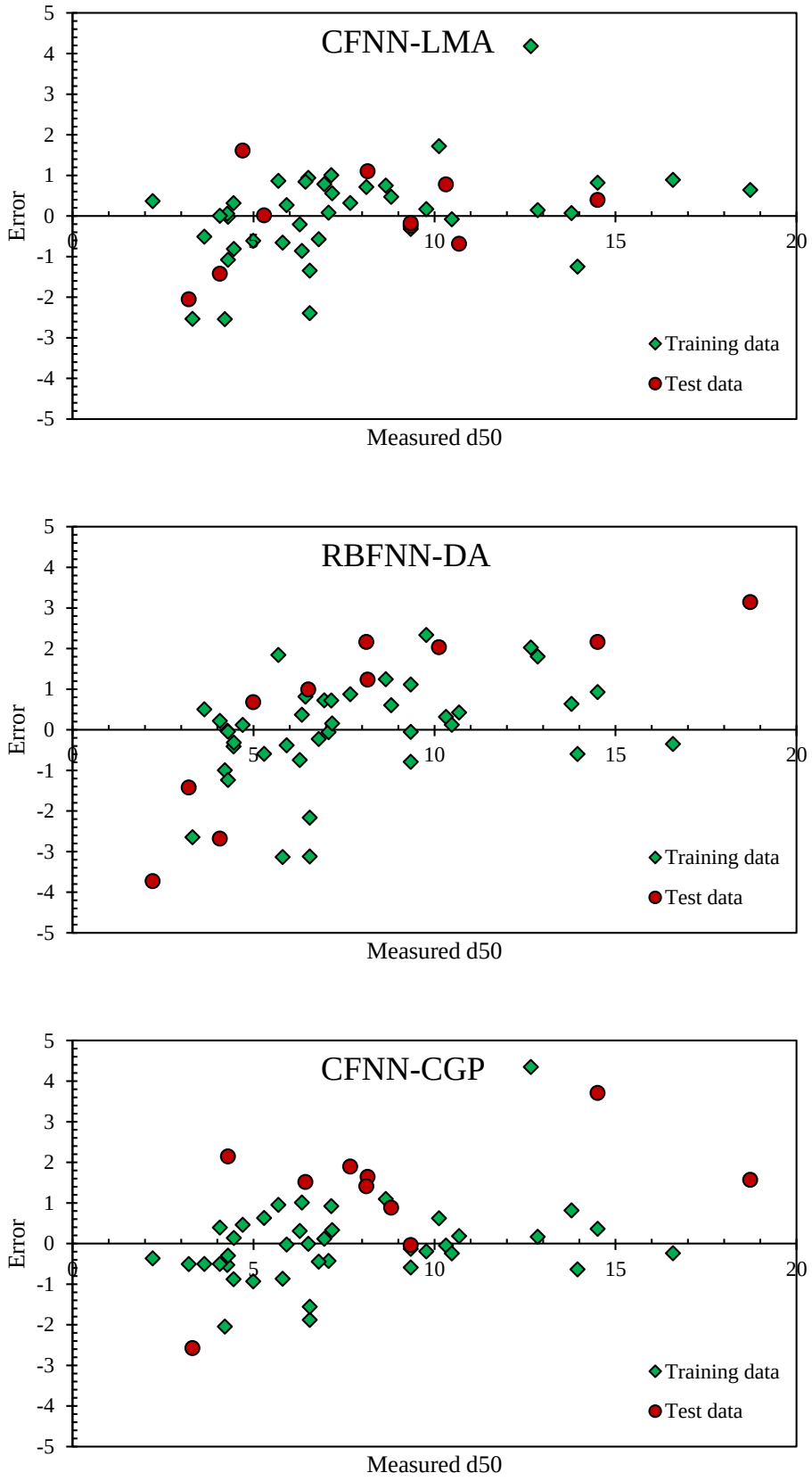

Fig. 6 Cross plots of the implemented CFNN and RBFNN schemes

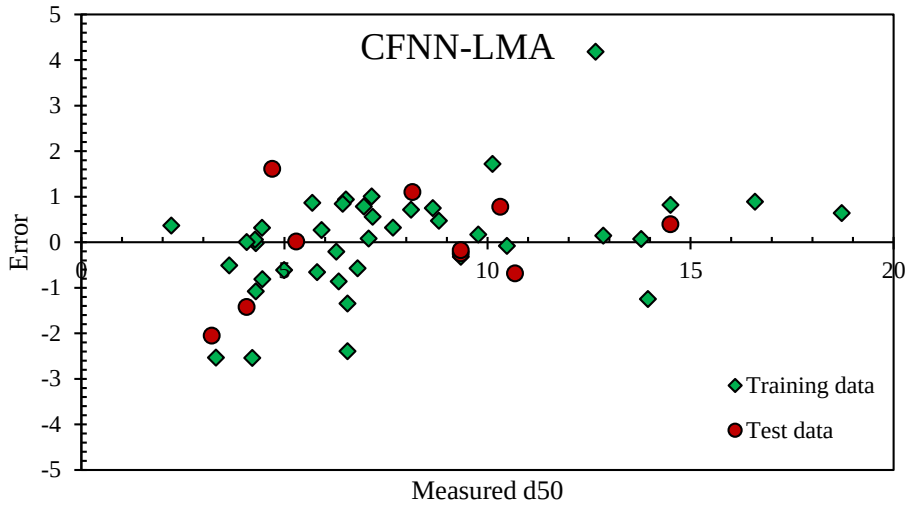

Fig. 6 Continued-

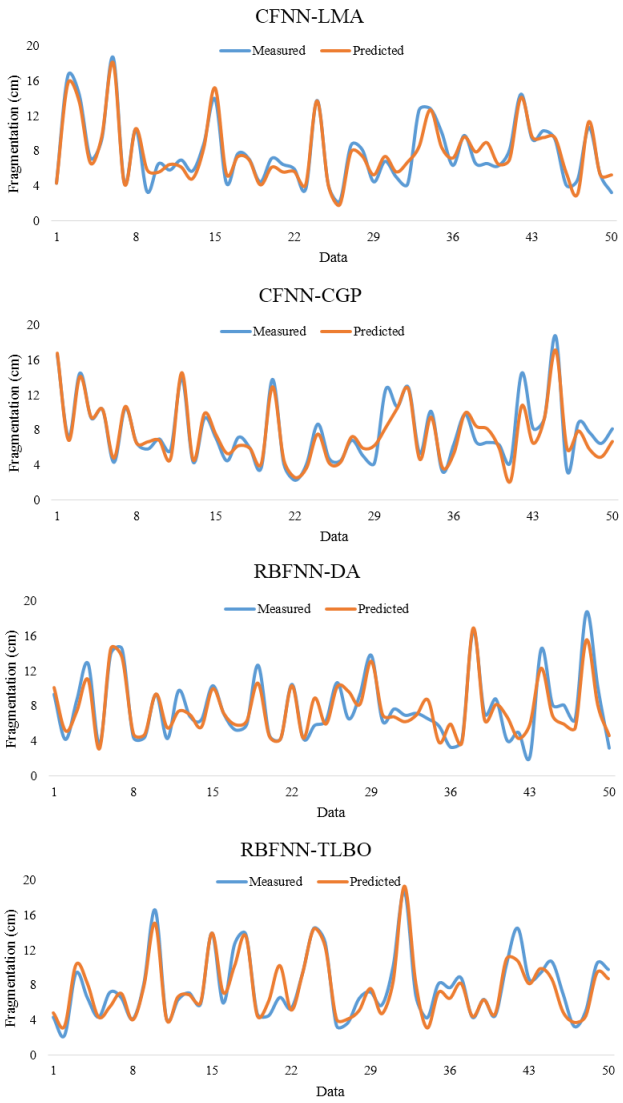

Fig. 7 Measured vs. predicted fragmentation values obtained from the developed models for all data

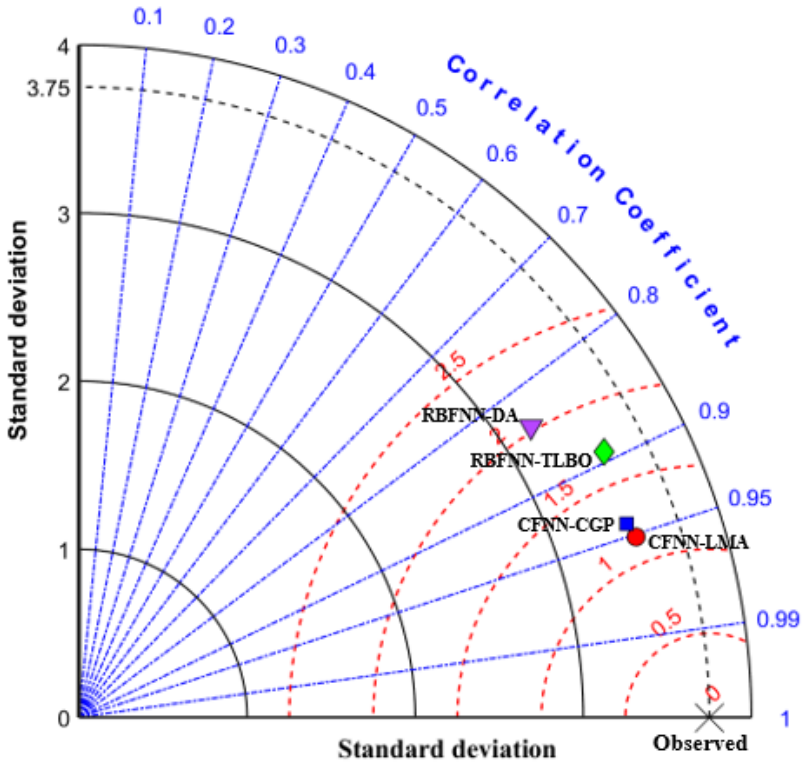

Fig. 8 Taylor diagram of the implemented CFNN and RBFNN schemes

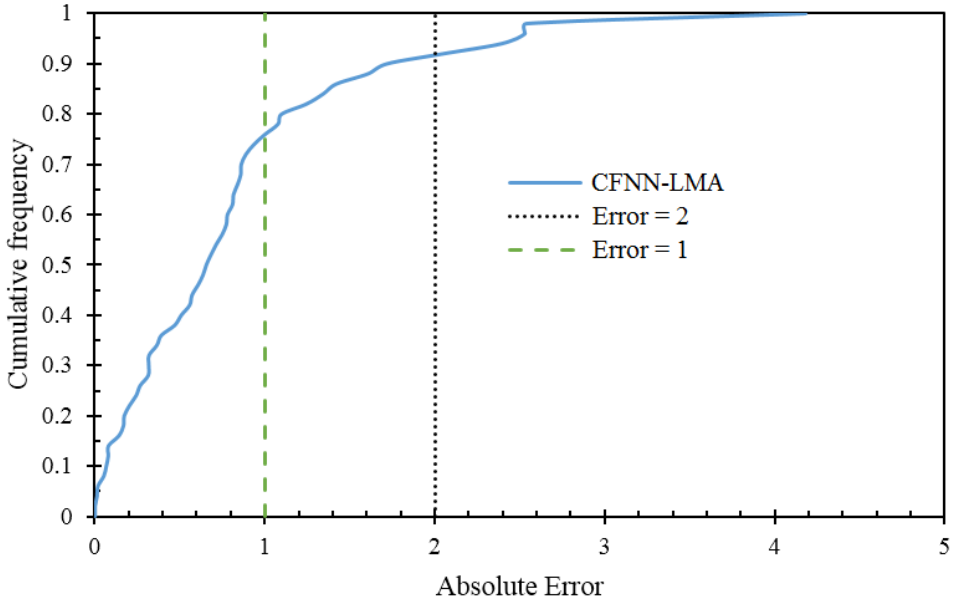

Fig. 9 Cumulative frequency of the absolute errors of the CFNN-LMA model

compared to the others. (2) According to the results of the sensitivity analysis, the rock properties parameters i.e., UCS, point load, hardness value, and density had the highest relevancy factor and were selected as the most impacting factors on the fragmentation values. And finally, (3) although the CFNN-LMA model proposed in this study worked accurately and effectively in predicting fragmentation in the studied cases, it could be applied to other sites depending on their own conditions.

Acknowledgments

This paper is supported by the National Natural Science Foundation of China (Grant No. 52174131).

References

Abujazar, M.S.S., Fatihah, S., Ibrahim, I.A., Kabeel, A. and Sharil, S. (2018), "Productivity modelling of a developed inclined

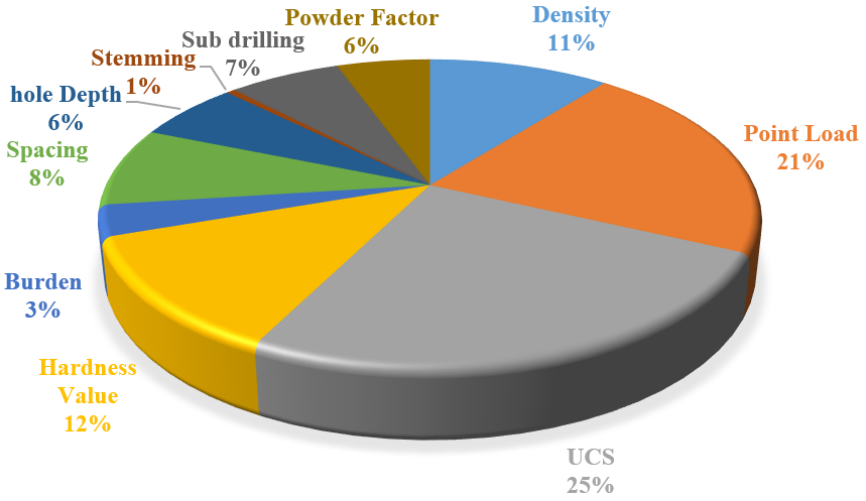

Fig. 10 Relevancy factor values of the sensitivity analysis evaluation

stepped solar still system based on actual performance and using a cascaded forward neural network model", *J. Cleaner Product.*. **170**, 147-159. https://doi.org/10.1016/j.jclepro.2017.09.092.

Apostolopoulou, M., Armaghani, D.J., Bakolas, A., Douvika, M.G., Moropoulou, A. and Asteris, P.G. (2019), "Compressive strength of natural hydraulic lime mortars using soft computing techniques", *Procedia Struct. Integrity*, **17**, 914-923. https://doi.org/10.1016/j.prostr.2019.08.122.

Armaghani, D.J., Asteris, P.G., Fatemi, S.A., Hasanipanah, M., Tarinejad, R., Rashid, A.S.A. and Huynh, V.V. (2020a), "On the use of neuro-swarm system to forecast the pile settlement", *Appl. Sci.*. **10**(6), https://doi.org/10.3390/app10061904.

Armaghani, D.J., Hatzigeorgiou, G.D., Karamani, C., Skentou, A., Zoumpoulaki, I. and Asteris, P.G. (2019), "Soft computing-based techniques for concrete beams shear strength", *Procedia Struct. Integrity*, **17**, 924-933. https://doi.org/10.1016/j.prostr.2019.08.123.

Armaghani, D.J., Mirzaei, F., Toghroli, A. and Shariati, A. (2020b), "Indirect measure of shear strength parameters of fiber-reinforced sandy soil using laboratory tests and intelligent systems", *Geomech. Eng.*, **22**(5), 397-414. https://doi.org/10.12989/gae.2020.22.5.397.

Asl, P.F., Monjezi, M., Hamidi, J.K. and Armaghani, D.J. (2018), "Optimization of flyrock and rock fragmentation in the tajareh limestone mine using metaheuristics method of firefly algorithm", *Eng. with Comput.*, **34**(2), 241-251. https://doi.org/10.1007/s00366-017-0535-9.

Asteris, P.G., Koopialipoor, M., Armaghani, D.J., Kotsonis, E.A. and Lourenço, P.B. (2021a), "Prediction of cement-based mortars compressive strength using machine learning techniques", *Neural Comput. Appl.*, **33**(19), 13089-13121. https://doi.org/10.1007/s00521-021-06004-8.

Asteris, P.G., Lourenço, P.B., Hajihassani, M., Adami, C.E.N., Lemonis, M.E., Skentou, A.D., Marques, R., Nguyen, H., Rodrigues, H. and Varum, H. (2021b), "Soft computing-based models for the prediction of masonry compressive strength", *Eng. Struct.*, **248**, 113276. https://doi.org/10.1016/j.engstruct.2021.113276.

Asteris, P.G., Mamou, A., Hajihassani, M., Hasanipanah, M., Koopialipoor, M., Le, T.T., Kardani, N. and Armaghani, D.J. (2021c), "Soft computing-based closed form equations correlating l and n-type schmidt hammer rebound numbers of rocks", *Transport. Geotech.*, **29**, 100588. https://doi.org/10.1016/j.trgeo.2021.100588.

Asteris, P.G., Nozhati, S., Nikoo, M., Cavaleri, L. and Nikoo, M. (2019), "Krill herd algorithm-based neural network in structural seismic reliability evaluation", *Mech. Adv. Mater. Struct.*, **26**(13), 1146-1153. https://doi.org/10.1080/15376494.2018.1430874..

Asteris, P.G., Skentou, A.D., Bardhan, A., Samui, P. and Lourenço, P.B. (2021d), "Soft computing techniques for the prediction of concrete compressive strength using non-destructive tests", *Constr. Build. Mater.*, **303**, 124450. https://doi.org/10.1016/j.conbuildmat.2021.124450.

Baghbani, A., Choudhury, T., Samui, P. and Costa, S. (2023), "Prediction of secant shear modulus and damping ratio for an extremely dilative silica sand-based on machine learning techniques", *Soil Dyn. Earthq. Eng.*, **165**, 107708. https://doi.org/10.1016/j.soildyn.2022.107708.

Bahadori, M. and Bakhshandeh Amnieh, H. (2018), "Implementation of hyperbolic tangent function to estimate size distribution of rock fragmentation by blasting in open pit mines", *Int. J. Min. Geo-Eng.*, **52**(2), 187-197. https://doi.org/10.22059/ijmge.2018.221013.594642.

Bahadori, M., Bakhshandeh Amnieh, H. and Khajezadeh, A. (2016), "A new geometrical-statistical algorithm for predicting two-dimensional distribution of rock fragments caused by blasting", *Int. J. Rock Mech. Min. Sci.*, **86**, 55-64. https://doi.org/10.1016/j.ijrmms.2016.04.002.

Bai, X.D., Cheng, W.C., Ong, D.E. and Li, G. (2021), "Evaluation of geological conditions and clogging of tunneling using machine learning", *Geomech. Eng.*, **25**(1), 59-73. https://doi.org/10.12989/gae.2021.25.1.059.

Bardhan, A., Gokceoglu, C., Burman, A., Samui, P. and Asteris, P.G. (2021), "Efficient computational techniques for predicting the california bearing ratio of soil in soaked conditions", *Eng. Geol.*, **291**, 106239. https://doi.org/10.1016/j.enggeo.2021.106239.

Bardhan, A. and Samui, P. (2022), "Probabilistic slope stability analysis of heavy-haul freight corridor using a hybrid machine learning paradigm", *Transport. Geotech.*, **37**, 100815, https://doi.org/10.1016/j.trgeo.2022.100815.

Benamara, C., Gharbi, K., Nait Amar, M. and Hamada, B. (2020), "Prediction of wax appearance temperature using artificial intelligent techniques", *Arabian J. Sci. Eng.*, **45**, 1319-1330. https://doi.org/10.1007/s13369-019-04290-y.

Bhandari, S. (1997), *Engineering Rock Blasting Operations*, A. A. Balkema, Rotterdam, Netherlands.

Cavaleri, L., Asteris, P.G., Psyllaki, P.P., Douvika, M.G., Skentou, A.D. and Vaxevanidis, N.M. (2019), "Prediction of surface treatment effects on the tribological performance of tool steels using artificial neural networks", *Appl. Sci.*, **9**(14). https://doi.org/10.3390/app9142788.

Chen, G., Fu, K., Liang, Z., Sema, T., Li, C., Tontiwachwuthikul, P. and Idem, R. (2014), "The genetic algorithm based back propagation neural network for MMP prediction in CO_2-EOR process", *Fuel.*, **126**, 202-212. https://doi.org/10.1016/j.fuel.2014.02.034.

Chen, H., Asteris, P.G., Jahed Armaghani, D., Gordan, B. and Pham, B.T. (2019), "Assessing dynamic conditions of the retaining wall: developing two hybrid intelligent models", *Appl. Sci.*, **9**(6), https://doi.org/10.3390/app9061042.

Cheng, M.Y. and Prayogo, D. (2017), "A novel fuzzy adaptive teaching–learning-based optimization (FATLBO) for solving structural optimization problems", *Eng. with Comput.*, **33**, 55-69. https://doi.org/10.1007/s00366-016-0456-z.

Chu, H., Yang, X., Li, S. and Liang, W. (2019), "Experimental study on the blasting-vibration safety standard for young concrete based on the damage accumulation effect", *Constr. Build. Mater.*, **217**, 20-27. https://doi.org/10.1016/j.conbuildmat.2019.05.070.

Dare-Bryan, P., Mansfield, S. and Schoeman, J. (2013). "Blast optimisation through computer modelling of fragmentation, heave and damage", *Proceedings of the Rock Fragmentation by Blasting: The 10th International Symposium on Rock Fragmentation by Blasting*, 2012 , Fragblast 10.

Dimitraki, L., Christaras, B., Marinos, V., Vlahavas, I. and Arampelos, N. (2019), "Predicting the average size of blasted rocks in aggregate quarries using artificial neural networks", *Bull. Eng. Geol. Environ.*, **78**, 2717-2729. https://doi.org/10.1007/s10064-018-1270-1.

Djordjevic, N. (1999). "A two-component model of blast fragmentation", *AusIMM Proceedings*, **304**(2), 9-13.

Ebrahimi, E., Monjezi, M., Khalesi, M.R. and Armaghani, D.J. (2016), "Prediction and optimization of back-break and rock fragmentation using an artificial neural network and a bee colony algorithm", *Bull. Eng Geol. Environ.*, **75**, 27-36. https://doi.org/10.1007/s10064-015-0720-2.

Elsharkawy, A.M. (1998). "Modeling the properties of crude oil and gas systems using RBF network", *SPE Asia Pacific oil and gas conference and exhibition*, https://doi.org/10.2118/49961-MS.

Esmaeili, M., Salimi, A., Drebenstedt, C., Abbaszadeh, M. and Aghajani Bazzazi, A. (2015), "Application of PCA, SVR, and ANFIS for modeling of rock fragmentation", *Arabian J. Geosci.*, **8**, 6881-6893. https://doi.org/10.1007/s12517-014-1677-3.

Fang, Q., Nguyen, H., Bui, X.N., Nguyen-Thoi, T. and Zhou, J. (2021), "Modeling of rock fragmentation by firefly optimization algorithm and boosted generalized additive model", *Neural Comput. Appl.*, **33**(8), 3503-3519. https://doi.org/10.1007/s00521-020-05197-8.

Gao, W., Karbasi, M., Hasanipanah, M., Zhang, X. and Guo, J. (2018), "Developing GPR model for forecasting the rock fragmentation in surface mines", *Eng. with Comput.*, **34**(2), 339-345. http://doi.org/10.1007/s00366-017-0544-8.

Gupta, V.K., Khani, H., Ahmadi-Roudi, B., Mirakhorli, S., Fereyduni, E. and Agarwal, S. (2011), "Prediction of capillary gas chromatographic retention times of fatty acid methyl esters in human blood using MLR, PLS and back-propagation artificial neural networks", *Talanta*, **83**(3), 1014-1022. https://doi.org/10.1016/j.talanta.2010.11.017.

Hasanipanah, M., Amnieh, H.B., Arab, H. and Zamzam, M.S. (2018), "Feasibility of PSO–ANFIS model to estimate rock fragmentation produced by mine blasting", *Neural Comput. Appl.*, **30**(4), 1015-1024. http://doi.org/10.1007/s00521-016-2746-1.

Hasanipanah, M., Jahed Armaghani, D., Bakhshandeh Amnieh, H., Majid, M.Z.A. and Tahir, M.M.D. (2017), "Application of PSO to develop a powerful equation for prediction of flyrock due to blasting", *Neural Comput. Appl.*, **28**(1), 1043-1050. https://doi.org/10.1007/s00521-016-2434-1.

Hasanipanah, M., Jahed Armaghani, D., Khamesi, H., Bakhshandeh Amnieh, H. and Ghoraba, S. (2016), "Several non-linear models in estimating air-overpressure resulting from mine blasting", *Eng. with Comput.*, **32**(3), 441-455. https://doi.org/10.1007/s00366-015-0425-y.

Haykin, S. (1999), *Neural Networks A Comprehensive Foundation*, BeiJing: Tsinghua University Press&Pren ─ 6ce HaJ1.

Haykin, S. (2009), *Neural Networks and Learning Machines*, Pearson Education India.

Hino, K. (1956), "Fragmentation of rock through blasting and shock wave theory of blasting", *Proceedings of the 1st US Symposium on Rock Mechanics (USRMS).*

Huang, J., Asteris, P.G., Manafi Khajeh Pasha, S., Mohammed, A.S. and Hasanipanah, M. (2022), "A new auto-tuning model for predicting the rock fragmentation: a cat swarm optimization algorithm", *Eng. with Comput.*, **38**(3), 2209-2220. https://doi.org/10.1007/s00366-020-01207-4.

Hustrulid, W. and Johnson, J. (2008). "A gas pressure-based drift round blast design methodology", *Proceedings of the 5th International Conference & Exhibition on Mass Mining*, Sweden, Lulea.

Hustrulid, W.A. (1999), *Blasting Principles for Open Pit Mining: General Design Concepts*, Balkema.

Iverson, S., Hustrulid, W., Johnson, J., Tesarik, D. and Akbarzadeh, Y. (2009). "The extent of blast damage from a fully coupled explosive charge", *Proceedings of the 9th International Symposium on Rock Fragmentation by Blasting*, (Fragblast-9).

Jimeno, C.L., Jimeno, E.L., Carcedo, F.J.A. and De Ramiro, Y.V. (1995), *Drilling and Blasting of Rocks*, CRC Press.

Johnson, J.C. (2010), *The Hustrulid Bar-A Dynamic Strength Test and its Application to the Cautious Blasting of Rock*, The University of Utah.

Kaloop, M.R., Bardhan, A., Samui, P., Hu, J.W. and Zarzoura, F. (2022), "Computational intelligence approaches for estimating the unconfined compressive strength of rocks", *Arabian J. Geosci.*, **16**(1), 37. https://doi.org/10.1007/s12517-022-11085-3.

Kanchibotla, S.S., Valery, W. and Morrell, S. (1999). "Modelling fines in blast fragmentation and its impact on crushing and grinding", *Proceedings of the Explo '99–A Conference on Rock Breaking*, The Australasian Institute of Mining and Metallurgy, Kalgoorlie, Australia.

Konya, C.J. and Walter, E.J. (1991), *Rock Blasting and Overbreak Control*, United States. Federal Highway Administration.

Länsivaara, T.T., Farhadi, M.S. and Samui, P. (2023), "Performance of traditional and machine learning-based transformation models for undrained shear strength", *Arabian J. Geosci.*, **16**(3), 183. https://doi.org/10.1007/s12517-022-11173-4.

Le, T.T., Skentou, A.D., Mamou, A. and Asteris, P.G. (2022), "Correlating the unconfined compressive strength of rock with the compressional wave velocity effective porosity and schmidt hammer rebound number using artificial neural networks", *Rock Mech. Rock Eng.*, **55**(11), 6805-6840. https://doi.org/10.1007/s00603-022-02992-8.

Li, C., Zhou, J., Khandelwal, M., Zhang, X., Monjezi, M. and Qiu, Y. (2022), "Six novel hybrid extreme learning machine–swarm intelligence optimization (ELM–SIO) models for predicting backbreak in open-pit blasting", *Natural Resour. Res.*, **31**(5), 3017-3039. https://doi.org/10.1007/s11053-022-10082-3.

Liu, L.L. and Wang, X.M. (2021), "Landslide susceptibility assessment using feature selection-based machine learning models", *Geomech. Eng.*, **25**(1), 1-16. https://doi.org/10.12989/gae.2021.25.1.001.

Menad, N.A. and Noureddine, Z. (2019), "An efficient methodology for multi-objective optimization of water alternating CO_2 EOR process", *J. Taiwan Inst. Chem. Engineers*, **99**, 154-165. https://doi.org/10.1016/j.jtice.2019.03.016.

Mirjalili, S. (2016), "Dragonfly algorithm: a new meta-heuristic optimization technique for solving single-objective, discrete, and multi-objective problems", *Neural Comput. Appl.*, **27**(4), 1053-1073. https://doi.org/10.1007/s00521-015-1920-1.

Mirjalili, S., Song Dong, J., Sadiq, A.S. and Faris, H. (2020), Genetic Algorithm: *Theory, Literature Review, and Application in Image Reconstruction*, Springer International Publishing, Cham. https://doi.org/10.1007/978-3-030-12127-3_5.

Moayedi, H., Abdullahi, M.a.M., Nguyen, H. and Rashid, A.S.A. (2021), "Comparison of dragonfly algorithm and Harris hawks optimization evolutionary data mining techniques for the assessment of bearing capacity of footings over two-layer foundation soils", *Eng. with Comput.*, **37**(1), 437-447. http://doi.org/10.1007/s00366-019-00834-w.

Morrell, S. (2004), "Predicting the specific energy of autogenous and semi-autogenous mills from small diameter drill core samples", *Minerals Eng.*, **17**(3), 447-451. http://doi.org/10.1016/j.mineng.2003.10.019.

Nait Amar, M. (2020), "Modeling solubility of sulfur in pure hydrogen sulfide and sour gas mixtures using rigorous machine learning methods", *Int. J. Hydrogen Energ.*, **45**(58), 33274-33287. https://doi.org/10.1016/j.ijhydene.2020.09.145.

Nait Amar, M., Jahanbani Ghahfarokhi, A., Ng, C.S.W. and Zeraibi, N. (2021a), "Optimization of WAG in real geological field using rigorous soft computing techniques and nature-inspired algorithms", *J. Petroleum Sci. Eng.*, **206**, 109038. https://doi.org/10.1016/j.petrol.2021.109038.

Nait Amar, M. and Zeraibi, N. (2019), "An efficient methodology for multi-objective optimization of water alternating CO2 EOR process", *J. Taiwan Inst. Chem. Engineers*, **99**, 154-165. https://doi.org/10.1016/j.jtice.2019.03.016.

Nait Amar, M., Ghriga, M.A., Ben Seghier, M.E.A. and Ouaer H. (2021b), "Predicting solubility of nitrous oxide in ionic liquids using machine learning techniques and gene expression programming", *J. Taiwan Inst. Chem. Engineers*, **128**, 156-168. https://doi.org/10.1016/j.jtice.2021.08.042

Nait Amar, M., Ghriga, M.A. and Ouaer, H. (2021c), "On the evaluation of solubility of hydrogen sulfide in ionic liquids using advanced committee machine intelligent systems", *J. Taiwan Inst. Chem. Engineers*, **118**, 159-168. https://doi.org/10.1016/j.jtice.2021.01.007.

Napier-Munn, T.J., Morrell, S., Morrison, R.D. and Kojovic, T. (1996), *Mineral Comminution Circuits: Their Operation And Optimisation*, Julius Kruttschnitt Mineral Research Centre, University of Queensland, Indooroopilly, Qld Australia.

Ouchterlony, F. (2005), "The Swebrec© function: linking fragmentation by blasting and crushing", *Min. Tech.*, **114**(1), 29-44. https://doi.org/10.1179/037178405X44539.

Pan, C.J., Tsai, M.C., Su, W.N., Rick, J., Akalework, N.G., Agegnehu, A.K., Cheng, S.-Y. and Hwang, B.-J. (2017), "Tuning/exploiting Strong Metal-Support Interaction (SMSI) in Heterogeneous Catalysis", *J. Taiwan Inst. Chem. Engineers*, **74**, 154-186. https://doi.org/10.1016/j.jtice.2017.02.012.

Rahimi, R. and Abdollahzade, A. (2020), "Study the process of self dilution in thickeners by computational fluid dynamics", *J. Anal. Numer. Method. Min. Eng.*, **9**(21), 33-42. https://doi.org/10.29252/anm.2019.8929.1311.

Rao, R.V., Savsani, V.J. and Vakharia, D.P. (2011), "Teaching–learning-based optimization: A novel method for constrained mechanical design optimization problems", *Comput.-Aided Design*. **43**(3), 303-315, http://doi.org/10.1016/j.cad.2010.12.015.

Shadab Far, M., Wang, Y. and Dallo, Y.A.H. (2019), "Reliability analysis of the induced damage for single-hole rock blasting", *Georisk: Assessment and Management of Risk for Engineered Systems and Geohazards*. **13**(1), 82-98, https://doi.org/10.1080/17499518.2018.1508728.

Skentou, A.D., Bardhan, A., Mamou, A., Lemonis, M.E., Kumar, G., Samui, P., Armaghani, D.J. and Asteris, P.G. (2023), "Closed-form equation for estimating unconfined compressive strength of granite from three non-destructive tests using soft computing models", *Rock Mech. Rock Eng.*, **56**(1), 487-514. https://doi.org/10.1007/s00603-022-03046-9.

Soltani-Mohammadi, S., Amnieh, H.B. and Bahadori, M. (2011), "Predicting ground vibration caused by blasting operations in Sarcheshmeh copper mine considering the charge type by adaptive neuro-fuzzy inference system (ANFIS)", *Archiv. Min. Sci.*, **56**(4), 701-710.

Sui Kim, I.T., Sethu, V., Arumugasamy, S.K. and Selvarajoo, A. (2020), "Fenugreek seeds and okra for the treatment of palm oil mill effluent (POME) – Characterization studies and modeling with backpropagation feedforward neural network (BFNN)", *J. Water Process Eng.*, **37**, 101500. https://doi.org/10.1016/j.jwpe.2020.101500.

Taylor, K.E. (2001), "Summarizing multiple aspects of model performance in a single diagram", *J. Geophys. Res.: Atmos.*, **106**(7), 7183-7192. http://doi.org/10.1029/2000JD900719.

Wyllie, D.C. and Mah, C. (2004), *Rock Slope Engineering*, CRC Press.

Xie, C., Nguyen, H., Bui, X.-N., Choi, Y., Zhou, J. and Nguyen-Trang, T. (2021), "Predicting rock size distribution in mine blasting using various novel soft computing models based on meta-heuristics and machine learning algorithms", *Geosci. Front.*, **12**(3). https://doi.org/101108, 10.1016/j.gsf.2020.11.005.

Zeng, J., Asteris, P.G., Mamou, A.P., Mohammed, A.S., Golias, E.A., Armaghani, D.J., Faizi, K. and Hasanipanah, M. (2021), "The effectiveness of ensemble-neural network techniques to predict peak uplift resistance of buried pipes in reinforced sand", *Appl. Sci.*, **11**(3). https://doi.org/10.3390/app11030908.

Zhou, J., Dai, Y., Khandelwal, M., Monjezi, M., Yu, Z. and Qiu, Y. (2021a), "Performance of hybrid SCA-RF and HHO-RF models for predicting backbreak in open-pit mine blasting operations", *Natural Resour. Res.*, **30**(6), 4753-4771. https://doi.org/10.1007/s11053-021-09929-y.

Zhou, J., Li, C., Arslan, C.A., Hasanipanah, M. and Bakhshandeh Amnieh, H. (2021b), "Performance evaluation of hybrid FFA-ANFIS and GA-ANFIS models to predict particle size distribution of a muck-pile after blasting", *Eng. with Comput.*, **37**(1), 265-274. https://doi.org/10.1007/s00366-019-00822-0.

Zhou, J., Qiu, Y., Khandelwal, M., Zhu, S. and Zhang, X. (2021c), "Developing a hybrid model of Jaya algorithm-based extreme gradient boosting machine to estimate blast-induced ground vibrations", *Int. J. Rock Mech. Min. Sci.*, **145**, 104856. https://doi.org/10.1016/j.ijrmms.2021.104856.

Zhou, J., Shen, X., Qiu, Y., Shi, X. and Khandelwal, M. (2022), "Cross-correlation stacking-based microseismic source location using three metaheuristic optimization algorithms", *Tunn. Undergr. Sp. Tech.*, **126**, 104570. https://doi.org/10.1016/j.tust.2022.104570.

Zimmermann, A.S. and Mattedi, S. (2020), "Density and speed of sound prediction for binary mixtures of water and ammonium-based ionic liquids using feedforward and cascade forward neural networks", *J. Molecular Liquids*, **311**, 113212. https://doi.org/10.1016/j.molliq.2020.113212.

CC